JGR Atmospheres

RESEARCH ARTICLE
10.1029/2018JD029368

# Observed and Simulated Teleconnections Between the Stratospheric Quasi-Biennial Oscillation and Northern Hemisphere Winter Atmospheric Circulation

**Martin B. Andrews[1], Jeff R. Knight[1], Adam A. Scaife[1,2], Yixiong Lu[3], Tongwen Wu[3], Lesley J. Gray[4], and Verena Schenzinger[5]**

[1]Hadley Centre, Met Office, Exeter, UK, [2]College of Engineering, Mathematics and Physical Sciences, University of Exeter, Exeter, UK, [3]National Climate Center, China Meteorological Administration, Beijing, China, [4]NCAS-Climate, Department of Physics, Oxford University, Oxford, UK, [5]Institute for Meteorology and Geophysics, University of Vienna, Vienna, Austria

**Key Points:**
- QBO teleconnection with the winter Arctic Oscillation is likely to be real, but observations only weakly constrain its strength
- Analysis using new deep QBO phase measure increases the strength and significance of the winter surface teleconnections
- Teleconnections between the deep QBO and Arctic Oscillation simulated by the HadGEM3 climate model are likely weaker than those observed

**Correspondence to:**
M. B. Andrews,
martin.andrews@metoffice.gov.uk

**Citation:**
Andrews, M. B., Knight, J. R., Scaife, A. A., Lu, Y., Wu, T., Gray, L. J., & Schenzinger, V. (2019). Observed and simulated teleconnections between the stratospheric Quasi-Biennial Oscillation and Northern Hemisphere winter atmospheric circulation. *Journal of Geophysical Research: Atmospheres*, *124*, 1219–1232. https://doi.org/10.1029/2018JD029368

Received 20 JUL 2018
Accepted 11 JAN 2019
Accepted article online 15 JAN 2019
Published online 1 FEB 2019



**Abstract** The Quasi-Biennial Oscillation (QBO) is the dominant mode of interannual variability in the tropical stratosphere, with easterly and westerly zonal wind regimes alternating over a period of about 28 months. It appears to influence the Northern Hemisphere winter stratospheric polar vortex and atmospheric circulation near the Earth's surface. However, the short observational record makes unequivocal identification of these surface connections challenging. To overcome this, we use a multicentury control simulation of a climate model with a realistic, spontaneously generated QBO to examine teleconnections with extratropical winter surface pressure patterns. Using a 30-hPa index of the QBO, we demonstrate that the observed teleconnection with the Arctic Oscillation (AO) is likely to be real, and a teleconnection with the North Atlantic Oscillation (NAO) is probable, but not certain. Simulated QBO-AO teleconnections are robust, but appear weaker than in observations. Despite this, inconsistency with the observational record cannot be formally demonstrated. To assess the robustness of our results, we use an alternative measure of the QBO, which selects QBO phases with westerly or easterly winds extending over a wider range of altitudes than phases selected by the single-level index. We find increased strength and significance for both the AO and NAO responses, and better reproduction of the observed surface teleconnection patterns. Further, this QBO metric reveals that the simulated AO response is indeed likely to be weaker than observed. We conclude that the QBO can potentially provide another source of skill for Northern Hemisphere winter prediction, if its surface teleconnections can be accurately simulated.

## 1. Introduction

Since the discovery of the stratospheric equatorial zonal wind QBO (Reed et al., 1961; Veryard & Ebdon, 1961), there have been ongoing efforts to understand the phenomenon and its influence on the Northern Hemisphere (NH) winter surface climate (see Baldwin et al., 2001 for a review). The QBO is equatorially confined to a latitude band of approximately 15°N to 15°S and exhibits alternating easterly and westerly zonal wind phases that descend from the equatorial upper stratosphere to the tropopause with a mean period of approximately 28 months (Baldwin et al., 2001), and periods ranging from 20 to 36 months. The downward progression of alternating QBO phases has occurred with almost unbroken regularity over the observational period. The only recorded exception occurred in the winter of 2015–2016, when the downward propagating westerly phase was interrupted by an easterly incursion (Newman et al., 2016; Osprey et al., 2016).

The influence of the QBO on the extratropical tropospheric winter circulation in observations was first assessed by Ebdon (1975) and confirmed by Holton and Tan (1980, 1982), who also provided evidence that the NH stratospheric polar vortex variability is dynamically linked to the QBO. A theory for the possible influence of the QBO on the extratropical atmosphere is based on the varying confinement of upward propagating tropospheric planetary waves and their interaction with the stratospheric zonal mean zonal wind. The zero wind line at 50 hPa varies from about 6°N to 20°N between the westerly (QBO-W) and easterly (QBO-E) phases, respectively. The location of the wind transition indicates a critical surface for

the absorption or reflection of equatorward propagating extratropical stationary (zero zonal phase speed) planetary waves. For QBO-E, therefore, more of the upward flux of planetary wave energy is confined to the Northern Hemisphere extratropics, favoring the disruption and weakening of the stratospheric polar vortex. Conversely, for QBO-W, these waves can achieve greater penetration into the equatorial regions, favoring a less perturbed and hence strengthened polar vortex (see Baldwin et al., 2001; Anstey & Shepherd, 2014 for reviews).

The strength of the NH winter stratospheric polar vortex is connected to changes in the principal pattern of atmospheric circulation variability in the troposphere, specifically in the Arctic Oscillation (AO; Thompson & Wallace, 1998). AO fluctuations have a marked effect on the surface weather across many parts of the Northern Hemisphere (Thompson & Wallace, 1998) including Europe (Thompson & Wallace, 2001). The AO also has a strong connection with the East Asian winter monsoon via the impact on the Siberian High (Gong et al., 2001). The East Asian winter monsoon is associated with temperature variations over eastern China. The North Atlantic Oscillation (NAO; Hurrell et al., 2003) is a regional equivalent of the AO and similarly has broad effects on European surface weather. Connections between the AO/NAO and the stratosphere in wintertime are a two-way interaction. The stratospheric polar vortex responds to tropospheric weather patterns via rapid upward planetary wave propagation (on a timescale of a day or two; e.g., Kodera et al., 2016). Changes in the stratospheric vortex, meanwhile, produce a slower downward influence (days to weeks; Baldwin & Dunkerton, 2001) that affects surface weather patterns, influencing the AO and NAO (Kidston et al., 2015). The most marked upheavals in the stratosphere, major sudden stratospheric warmings (Scherhag, 1952) involve the temporary collapse of the winter polar vortex and show a subsequent lagged effect on the troposphere (Kolstad et al., 2010). The typical surface response to such events is a negative phase of the AO and NAO, which can result in easterly winds bringing cold air outbreaks in Western Europe and the Eastern United States. While the teleconnection between the QBO and surface conditions in the wintertime extratropical Northern Hemisphere is most often considered as being mediated via the polar stratospheric vortex (Holton & Tan, 1980), alternative routes are an ongoing topic of interest (see, e.g., Figure 1 of Gray et al., 2018, and references therein). These include a proposed impact of the QBO-induced meridional circulation on the subtropical jet (Garfinkel & Hartmann, 2011; Ruti et al., 2006; Simpson et al., 2009) and the direct impact of the QBO on the underlying deep convection at tropical latitudes, which then influences the generation of large-scale planetary waves that propagate into the midlatitudes (Liess & Geller, 2012; Gray et al., 2018).

Demonstrating a QBO-AO teleconnection in observations is complicated by the limited duration of the QBO record, which restricts our ability to overcome confounding influences on the polar vortex and mean sea level pressure (MSLP) patterns. These competing influences include solar variability (Andrews et al., 2015; Gray et al., 2010, 2013, 2016; Ineson et al., 2011; Scaife et al., 2013), tropical volcanic eruptions which inject radiatively active aerosols into the stratosphere (Driscoll et al., 2012; Stenchikov et al., 2004), El Niño–Southern Oscillation (Bell et al., 2009), and chaotic internal variability. An alternative approach is therefore to examine the QBO-surface teleconnections in global climate model simulations with realistic internally generated QBO variability. Simulations over much longer periods than is covered by the observational record are available with such models, extending in many cases to hundreds of years. Of course, the price of using models is that they may contain errors or omissions in the simulation of the QBO or its teleconnections. Nevertheless, if the simulations reproduce aspects of the observed surface teleconnections, they can provide supporting evidence that these connections are real and not an artifact of sampling over the short observational record.

Numerous studies have examined the NH winter surface response to the phase of the QBO using climate models. For example, Marshall and Scaife (2009) assessed the winter surface response to the QBO at 30 hPa using two versions of an atmosphere-only global climate model differing in vertical resolution and domain in seasonal hindcast experiments. They found a weaker stratospheric polar vortex for QBO-E than for QBO-W, and a negative AO-like response in the surface temperature field. The surface temperature patterns they obtained are also indicative of an NAO-like response to the QBO. Given that the QBO itself is fairly predictable more than three years ahead (Scaife, Arribas, et al., 2014; Scaife, Athanassiadou, et al., 2014), the inference is that there is some forecast skill to be gained providing that (a) the QBO teleconnection with the NH winter surface is real and (b) models are able to reproduce this teleconnection.

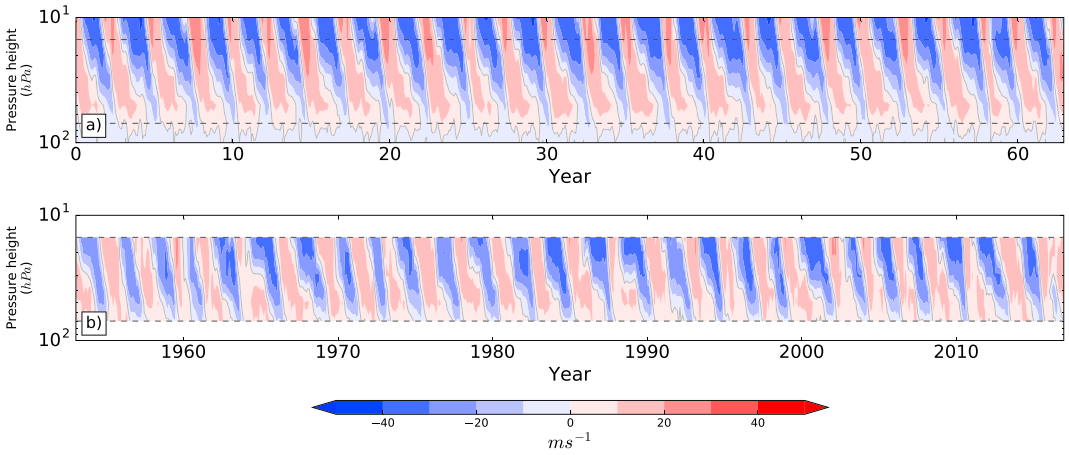


**Figure 1.** Hovmöller diagram showing (a) a sample of the spontaneously generated equatorial zonal mean zonal wind evolution over a 63-year period of the simulation (approximately one fifth of the total simulation length) and (b) the zonal wind evolution of the FUB observational data set 1953–2016. The 10-hPa data from the FUB data set are not plotted as they do not cover the entire period, but are available from 1956 onward. The 15- and 70-hPa levels are marked with horizontal dashed lines to aid comparison.

In this study, we use a multicentury preindustrial control simulation produced with a coupled climate model to explore the influence of the QBO on winter NH extratropical climate. The benefit of using a long control simulation to examine the teleconnections is that the climate is stable (i.e., not drifting), and free from external influences (such as solar variability and volcanic eruptions) that could confound an estimate of the magnitude of the teleconnections between the QBO and the AO or NAO. In addition, the length of the simulation allows the QBO influence to be more confidently isolated from the effects of El Niño–Southern Oscillation and internal noise, as aliasing is minimized in a long simulation.

Previous studies have tended to analyze the QBO in terms of a single-level QBO index. This may not reflect the vertical structure of the QBO, however, which could be important for the extratropical surface response. Pascoe et al. (2006) examined the impact of the vertical structure of the QBO in atmosphere-only experiments where the equatorial stratosphere was relaxed to idealized shallow or deep QBO winds, both including the semiannual oscillation (see Pascoe et al., 2006, Figure 1). They demonstrated that the simulated response to a deep QBO is to bring forward the onset of midwinter sudden stratospheric warmings, similar to the signal in observations (Dunkerton et al., 1988; Gray et al., 2018). This result suggests the possibility that the height structure of the QBO could be an important factor both in influencing sudden stratospheric warmings and the surface AO/NAO indices. This was indeed found to be the case in the recent study of Schenzinger (2017) who employed an empirical orthogonal function (EOF) approach to characterize the height structure (see also Gray et al., 2018). To address this possibility we will use two types of QBO index. The first is a single-level QBO index derived as the zonal mean zonal equatorial wind at 30 hPa, as adopted in numerous previous studies. The second is a phase-angle calculated in the space of equivalent indices from two levels to explore the impact of the vertical structure of the QBO.

## 2. Methods

We employ a model simulation with a duration of 313 years using the atmosphere–ocean-land-sea ice coupled climate model HadGEM3-GC2 (Williams et al., 2015). The model atmospheric resolution is approximately 60 km in midlatitudes with 85 quasi-horizontal levels from the surface up to 85 km. The Nucleus for European Modeling of the Ocean version 3.4 ocean model (Madec, 2008) is used with a nominal horizontal resolution of 0.25° and 75 levels. Coupling is achieved using Ocean Atmosphere Sea Ice Soil model version 3 (Valcke, 2010) and is performed every 3 hr. The model has a realistic internally generated QBO (Figure 1a), which is partly driven by waves resolved by the model, and partly by parameterized non-orographic gravity waves (Scaife et al., 2002). The preindustrial control simulation is initialized from the end of a 133-year-long spin-up integration and has a stable long-term climate (the global annual mean surface temperature drift is +0.05 K/century). It uses Coupled Model Intercomparison Project phase 5 forcings (Jones et al., 2011)

appropriate to circa 1850. Total Solar Irradiance is specified as the average over the period of two solar cycles from 1850 to 1882 and stratospheric volcanic aerosols are set to background levels (Sato et al., 1993).

We compare the analysis of the simulation with observations (over the period from 1953 to 2016) using the MSLP data set from the National Centers for Environmental Prediction/National Center for Atmospheric Research Reanalysis-1 (Kalnay et al., 1996) and the equatorial stratospheric wind radiosonde observational data set (Figure 1b) available from the Freie Universität Berlin (FUB; Kunze, 2017). The observation-based QBO indices are generated using the FUB data set.

The simulated QBO at 30 hPa has a mean period of 30.4 months and a range of 23–35 months. This compares reasonably well with the observed QBO, which has a mean period of 27.8 months, and a range of 20–36 months. The mean maximum wind speed and standard deviation of peak winds in the simulation for QBO-W are 20.4 and 1.9 $ms^{-1}$, respectively, and for QBO-E, −28.3 and 2.3 $ms^{-1}$. The equivalent FUB values are, for QBO-W, 16 and 2.7 $ms^{-1}$, and for QBO-E, −31.3 and 3.0 $ms^{-1}$. The simulated and observed QBO are similar in magnitude and standard deviation.

For this study, we use two different winter (December-January-February) QBO indices. The initial analysis employs a single-level QBO index defined as the near-equatorial zonal mean zonal wind at 30 hPa, which is a common definition used by previous studies (e.g., Marshall & Scaife, 2009; Scaife, Arribas, et al., 2014; Scaife, Athanassiadou, et al., 2014) and is the closest available model diagnostic to lower indices, typically ~40 hPa used in other observational and modeling studies to optimize extratropical correlations (e.g., Dunkerton & Baldwin, 1991; Hamilton, 1998). We considered using a QBO index at 50 hPa, but found that the AO and NAO responses are very weak. For observations the QBO index is taken as the 30-hPa zonal wind from the FUB data set, and for the model simulation is calculated as the area-averaged zonal winds between 5°N and 5°S at 30 hPa. A threshold of ±5 $ms^{-1}$ is applied to the QBO index when making composites of MSLP for QBO-W minus QBO-E conditions to remove neutral cases.

Further analysis to explore the impact of the vertical structure of the QBO requires an alternative method of sampling the QBO to be defined. Other studies have attempted this, typically relying on the calculation of the first and second EOFs (Dunkerton, 2017; Fraedrich et al., 1993; Gray et al., 2018; Wallace et al., 1993). The principal components of these EOFs define a space in which a QBO amplitude and phase can be obtained (Schenzinger, 2017).

The peaks of the first two EOFs of the QBO vertical wind profiles, identified by Wallace et al. (1993), Fraedrich et al. (1993), Dunkerton (2017), and Gray et al. (2018), occur at approximately 15 and 30 hPa. These levels span the range over which the QBO tends to propagate steadily downward, and are above the level where the QBO-E phase can "stall." The vertical separation is large enough to discriminate between deeper and shallower QBO vertical structure. For example, when both levels are westerly (easterly), the equatorial middle stratosphere is entirely westerly (easterly). If the vertical separation is increased by changing the lower index from 30 to 50 hPa, the slower descent of the easterly shear zone compared to the westerly shear zone results in no deep easterlies, making analysis impractical. We choose QBO indices at 15 and 30 hPa, from the available levels in the observational and simulation data sets, to represent the vertical structure of the QBO in the middle stratosphere.

The December-January-February MSLP data sets from the reanalysis and the simulation are detrended to remove any residual long-term trends, as are the QBO indices. The AO is calculated simply as the difference in surface pressure of the area-weighted zonal means for the bands 30°N–60°N, and 60°N–90°N. The NAO is calculated as the difference in surface pressure between the Azores and Iceland.

## 3. Analysis

### 3.1. QBO Teleconnections in Observations and Model Simulation

First, we assess the winter (December-January-February) MSLP response to the QBO in observations, by examining the difference between the means of MSLP composites of winters with QBO-W and QBO-E.

The observed MSLP response in the winter hemisphere (Figure 2a) exhibits a clear pattern of negative pressure anomalies in the polar region and positive anomalies in midlatitudes. This annular pattern projects positively onto the AO, with an AO anomaly of +1.3 hPa (~0.4 σ). The main regions of significance lie

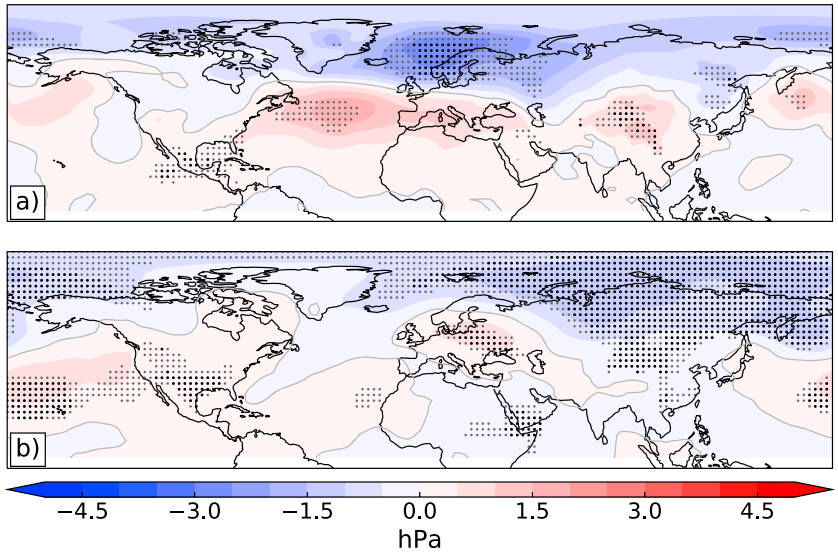


**Figure 2.** Winter (DJF-mean) MSLP composite response to QBO-W minus QBO-E for (a) NCEP-NCAR MSLP reanalysis using the FUB QBO data set at 30 hPa (23 winters for QBO-W, and 25 for QBO-E) and (b) the control simulation (144 winters for QBO-W, and 131 for QBO-E). Regions significant at the 90 and 95% one-sided confidence level are marked with gray and black stippling, respectively.

over the North Atlantic and Scandinavia with the positive and negative nodes shifted westward and eastward, respectively, in relation to the climatological NAO pattern. Nevertheless, the pattern projects positively onto the station-based NAO index, producing an NAO anomaly of +3.1 hPa (~0.3 σ). There is also a significant positive MSLP anomaly over China.

To analyze whether the MSLP response is significant, a Monte Carlo approach is adopted. We randomly sample winters from the observational data set, compositing numbers of winters that correspond in size to the number of QBO-W and QBO-E samples (23 for QBO-W and 25 for QBO-E). The expectation of the difference between the means of this pair of MSLP composites is clearly zero by construction. Repeating this 1,000 times, therefore, gives the distribution of differences expected by chance when selecting winters in the way we have done for the QBO composite. We assess the magnitude of the QBO composite difference to be significant where it exceeds that of 90 and 95% of the randomly generated distribution (see stippling in Figure 2a), using a one-sided test criteria, which correspond to 80 and 90% significance levels of a two-sided test. This shows that significance is found for the main centers of action of the difference pattern, but not more generally across the middle and high latitudes.

The MSLP response to the QBO simulated by the HadGEM3 model is shown in Figure 2b. The simulated winter AO and NAO standard deviations, 2.9 and 8 hPa, respectively, are similar to those observed. Compared with observations, the simulated MSLP winter response to QBO-W minus QBO-E exhibits a broadly similar positive-AO pattern, but is of weaker amplitude. Despite this, the large number of winters making up the composites (144 for QBO-W and 131 for QBO-E) ensures grid-point level significance over most of the pattern, since chance differences are averaged out. Unlike the QBO effect estimated from observations, however, the pattern has little focus on the North Atlantic sector and the response over China is of opposite sign.

The Monte Carlo approach is also applied to the AO and NAO large-scale circulation indices (Figure 3). For the QBO-AO teleconnection in observations (Figure 3a), the distribution of mean AO differences is computed for 1,000 randomly resampled pairs of composites of the same size as the numbers of QBO-W and QBO-E winters (23 and 25, respectively). As stated above, the expectation value of the difference is zero by construction, and this is confirmed by the computed distribution, which is symmetric about zero. The range of differences possible from random sampling of the AO has a ±2 standard deviation width of about ±1.5 hPa. The difference between the means of the QBO-W and QBO-E AO composites derived from

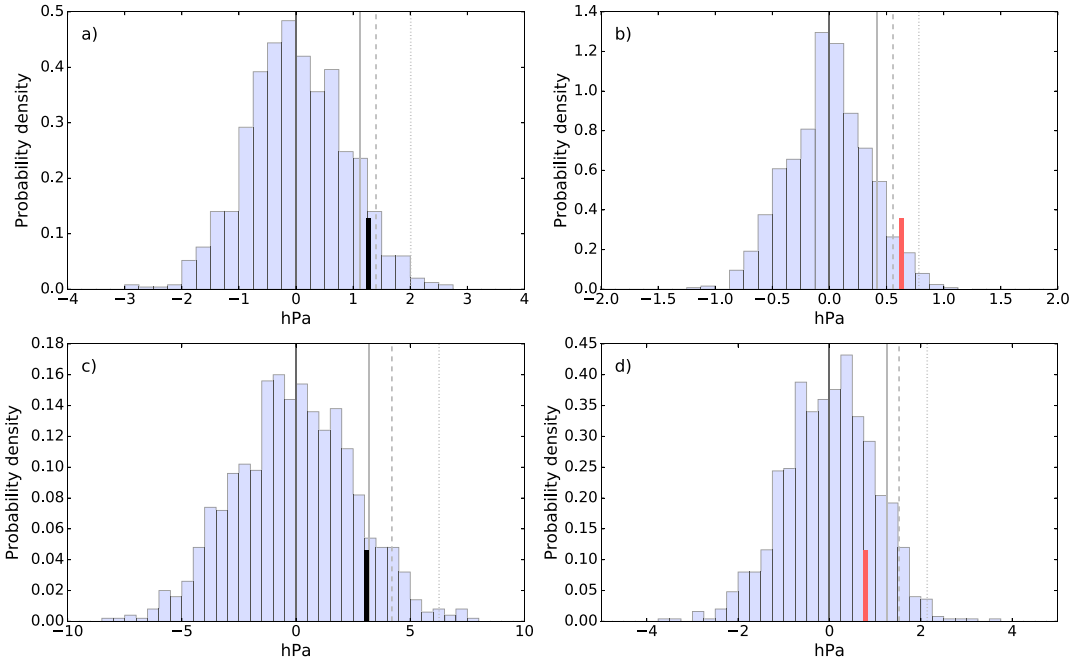


**Figure 3.** Distribution of winter AO and NAO responses based on 1,000 sampling iterations, not conditioned on QBO phase. The observational distributions are shown in (a) and (c) for the AO and NAO, respectively, and for the simulation distributions, in (b) and (d), respectively. The black vertical lines show the observed winter response to QBO index at 30-hPa westerly minus easterly phases, and the red vertical lines the equivalent model response. The vertical gray lines identify one-sided significance thresholds of 90% (solid), 95% (dashed), and 99% (dotted).

observations is +1.3 hPa (black vertical line on diagram). Thus, the observed AO response to the QBO is significant at the 90% level, but not at the 95% level.

The resampled range of AO differences from the HadGEM3 simulation is shown in Figure 3b. Here the number of winters in each pair of resampled composites (144 and 131) is much larger than is available for the reanalysis. This reduces the residual variability in the difference of the means of the random samples, giving a width of just under ±0.6 hPa for the distribution. The mean AO index for the QBO-W minus the QBO-E composite is just over +0.6 hPa (red vertical line on diagram). Although this is smaller than the value derived from observations, it is statistically significant at the 95% level due to the greater ability of the long simulation to discriminate a signal from the effects of random noise. The combination of results from the model with those from observations gives more confidence that the QBO has an impact on the AO.

The variability of the NAO is greater than that of the AO in both the observations and the model simulation, and as a result, the residual variability in the resampled differences is also larger (±4.2 hPa in observations and ± 1.5 hPa in the model; see Figures 3c and 3d). The QBO composite shows a mean value of +3.1 hPa for the station-based NAO (Figure 3c). This is close to the 90% significance level. The weaker significance for the NAO appears to relate to the shifts in the nodes of the QBO-related pattern from the conventional nodes of the NAO. For the simulation, the inferred NAO response to the QBO is only +0.8 hPa and is not statistically significant. As this small value could very plausibly be an artifact of sampling simulated NAO variability, this analysis does not detect a robust influence of the QBO on the NAO in the model.

In summary, the statistical confidence levels revealed by resampling show that the existence of a QBO influence on the AO is likely, and for the NAO is probable but not certain. The relative shortness of the observational period is shown to be a challenge for the detection of QBO signals. The much longer model simulation shows a statistically significant AO response but the NAO response suggested by observations is not detected. Further, the amplitude of the simulated teleconnections appears to be considerably smaller than observed—half the size or less in both cases. An obvious potential cause for this is a deficiency in the simulated QBO teleconnection. As has been shown here, however, sampling of the AO and NAO over a relatively short period can produce residuals unrelated to the QBO. An alternative explanation, therefore, is that sampling coincidental variability artificially inflates the estimate of the QBO influence over the observational

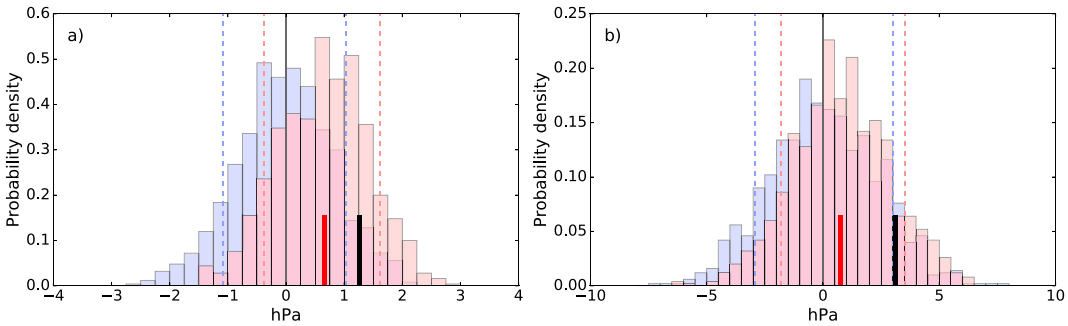


**Figure 4.** Distributions of simulated winter (a) AO and (b) NAO generated using the sample sizes from observations (23 winters for QBO-W and 25 for QBO-E). The blue distributions are not conditioned on the QBO phase at 30 hPa, whereas the pink distributions are. Black vertical lines signify the QBO-W minus QBO-E signal in observations, and the red vertical lines signify the model medians for QBO-W minus QBO-E. The blue (pink) dashed lines signify the 10–90% distribution thresholds for the blue (pink) model distributions.

period or decreases it in the model. The analysis in Figure 3 is not able to distinguish between these alternatives, so in the next section we analyze the consistency of the simulation and the reanalysis by creating subsamples from the simulation with the same number of winters as in the reanalysis.

### 3.2. Consistency of the Model With Observations

It has been shown above that the probability of the observed teleconnections being artifacts of sampling variability unrelated to the QBO is sufficient to prevent us from entirely ruling this possibility out (Figures 3a and 3c). Similarly, estimated magnitudes of QBO-induced changes in the observations are also subject to sampling uncertainty, hampering robust comparisons with the model. One way to estimate the uncertainty in the observed teleconnections is to subsample the much longer model simulation, since it contains many potential analogues of the observational QBO-W and QBO-E composites. This is justified as the overall AO and NAO variability is very similar in the model and observations (Scaife, Arribas, et al., 2014; Scaife, Athanassiadou, et al., 2014), so sampling the simulated variability is expected to give a similar spread to resampling the observations.

To achieve this, we select sets of pairs of samples with and without conditioning the selection on the phase of the QBO. The distributions derived for the AO are plotted in Figure 4a. As expected, this shows that the distribution of random (i.e., not conditioned on the phase of the QBO) composite differences is centered on zero and has a very similar width to the distribution derived from observations (Figure 3a). This validates our approach in sampling the model as an estimate of the uncertainty in the observed teleconnection. In addition, the distribution that is conditioned on the QBO shows a clear positive difference in the composite mean of +0.6 hPa, consistent with the mean QBO-W minus QBO-E value found over the whole multicentury simulation. The distribution conditioned on the QBO phase shows that, despite the small mean AO value, individual samples with the same number of QBO-W and QBO-E winters as the observations can produce an AO response between approximately −0.3 and +1.6 hPa (10th to 90th percentile). Crucially, this range includes the observed AO index of +1.3 hPa, meaning that pairs of QBO-W and QBO-E composites with a similar mean MSLP difference can be found reasonably frequently in the simulation. The fact the amplitude of the simulated QBO-AO teleconnection is much smaller than observed means we cannot conclude it is unrealistic, since it is possible that the difference is due to sampling over the relatively short observational period. Therefore, two possibilities remain: first that the model simulates the teleconnection correctly and the teleconnection estimated from observations is inflated by sampling of independent variability or second that the model genuinely produces an unrealistically weak teleconnection. The results here show that for the QBO and AO metrics we have used it is not possible to distinguish between these alternatives. Only a longer observational data set, allowing more confident estimation of the observed teleconnection, could remedy this.

Compared to the AO distributions, the NAO distributions (Figure 4b) show much less of a shift between the unconditioned and conditioned distributions of composite differences, consistent with the very small signal in the model (0.7 hPa). Again, the distribution of the unconditioned values matches the distribution from resampling the observations (Figure 3c) very well. The 10th to 90th percentile range of NAO composite differences in the conditional distribution is −1.8 to +3.5 hPa, which just encompasses the QBO teleconnection

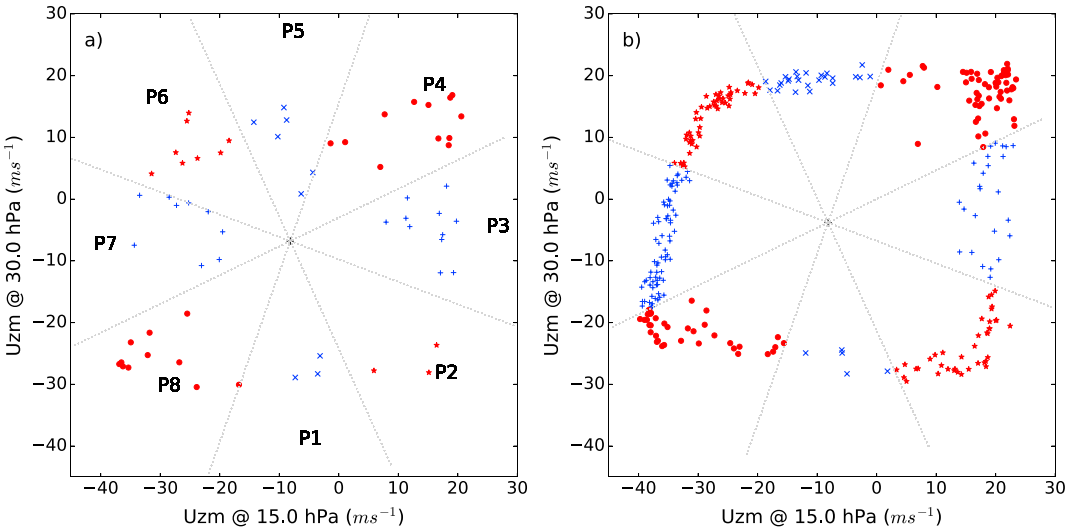


**Figure 5.** Scatterplot of winter QBO indices at the 15- versus 30-hPa levels for (a) observations and (b) the simulation. Lines radiating from the anomaly center indicate the separation of phases P1 through P8. Symbols and colors provide visual identification of the points that fall into each of the phases.

estimated from observations (+3.1 hPa). Despite the apparently very marked difference between the NAO response to the QBO in observations and the model, therefore, proof of a discrepancy remains very marginal. This shows that with the size of the signals found and the levels of variability inherent in observations, the 63 years of observations available is too short to evaluate the faithfulness of the model's teleconnections with the QBO.

### 3.3. Surface Response to Deep QBO Phases

The difficulty in evaluating the model against a relatively short observational record highlighted in the previous section might indeed be an insurmountable issue (at least until a longer record is available). On the other hand, it could be the case that other metrics of the QBO would allow greater discrimination between

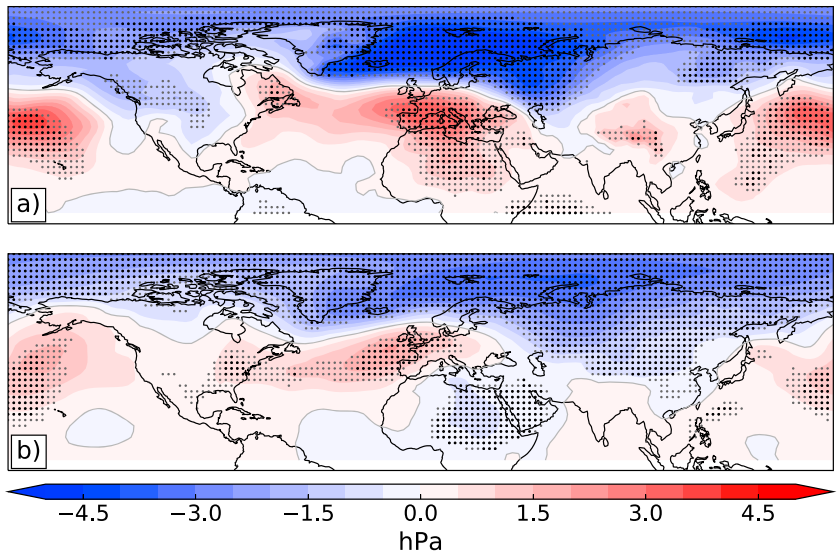


**Figure 6.** MSLP composite response to P4 minus P8 winters for (a) observations (12 winters for deep-QBO-W, and 11 for deep-QBO-E) and (b) the control simulation (59 winters for deep-QBO-W, and 35 for deep-QBO-E). Regions significant at the 90 and 95% one-sided confidence level are marked with gray and black stippling, respectively.

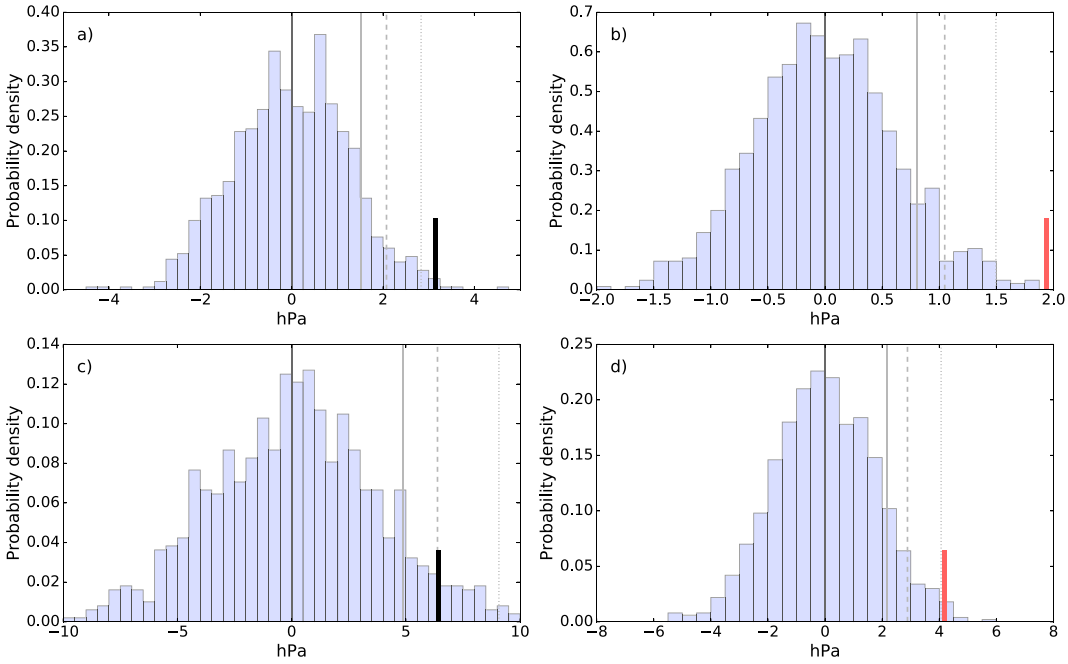


**Figure 7.** Same as in Figure 3 but exploring the variability and significance of P4 minus P8 winters. The observational distributions are shown in (a) and (c) for the AO and NAO, respectively, and for the simulation distributions, in (b) and (d), respectively.

observed and simulated teleconnections. Here we follow the recent study of Schenzinger (2017) and Gray et al. (2018) by choosing to examine an alternative description of the QBO aimed at capturing the evolution of the vertical structure of the zonal wind. We employ QBO indices at two levels, 15 and 30 hPa, to capture the height profile of the equatorial winds in the middle stratosphere. The variation of the QBO in the space spanned by these indices for the observations and the model simulation is shown in Figure 5. We segment the phase space into eight phases (labeled in Figure 5a) to allow the QBO phases with deep westerly and easterly profiles to be distinguished from intermediate phases which contain a descending QBO shear zone at intermediate levels. Each sector is 45° in width, and rotated with respect to the axes to maximize the number of observed samples in the deep QBO phases (P4, P8). Both the observations (Figure 5a) and the model simulation (Figure 5b) show similar distributions, in which the points trace the path of an counterclockwise orbital trajectory from phase P1 through to P8. This corresponds to the downward progression of QBO phases (see, for example, a similar representation of phase descent in Figure 2 of Gray et al., 2018). As the westerly phase first appears at 15 hPa (P2), the zonal wind at 30 hPa is easterly. Over time, the 30-hPa wind transitions to westerly, such that the QBO is westerly over the whole of the range between the two levels (P4). The 15-hPa zonal wind then declines at the onset of the subsequent easterly phase (P6) before this transition propagates down to the 30-hPa level (P8).

**Table 1**
*Number of Samples and Associated AO and NAO Indices for Each Phase-Pair Composite Difference From Observations*

| Phase Pair Difference | Number of Samples ($P_x$, $P_y$) | AO (hPa) | NAO (hPa) |
|---|---|---|---|
| P4 − P8 | 12, 11 | **3.15** | ***6.44*** |
| P5 − P1 | 6, 3 | −1.92 | −3.59 |
| P6 − P2 | 8, 3 | 0.91 | 2.14 |
| P7 − P3 | 9, 11 | −0.05 | 1.20 |

*Note.* Numbers highlighted in bold are significant above the 99% threshold, and in bold-italic, above the 95% threshold.

We now consider the difference of phases P4 and P8, that is, deep westerly QBO minus deep easterly QBO winters, as it was noted by Gray et al. (2018) that the maximum MSLP response is found when the QBO has similarly signed anomalies over an extended depth (see their Figure 7). Here the number of winters in each pair of resampled composites for deep QBO-W and deep QBO-E is 12 and 11, respectively, for observations, and 59 and 35, respectively, for the simulation. The observed and simulated winter MSLP responses (Figure 6) show notable similarities in the NH, much more so than when using just the QBO index at 30 hPa (Figure 2). Furthermore, both appear considerably stronger and more statistically significant than their counterparts inferred using the single-level index at 30 hPa. Interestingly, the model again shows a weaker response.

**Table 2**
*Same as in Table 1 but for the Simulation*

| Phase Pair Difference | Number of Samples ($P_x$, $P_y$) | AO (hPa) | NAO (hPa) |
|---|---|---|---|
| P4 − P8 | 59, 35 | **1.94** | **4.19** |
| P5 − P1 | 25, 5 | 0.07 | 0.88 |
| P6 − P2 | 50, 39 | −0.08 | −0.67 |
| P7 − P3 | 75, 25 | 0.47 | 0.26 |

*Note.* Numbers highlighted in bold are significant above the 99% threshold.

A particularly notable feature is the dipole over the North Atlantic in the simulation that is missing from the results of the single-level analysis, and which projects positively onto the NAO.

The observed and simulated mean AO for QBO composites of phase P4 minus composites of phase P8 are +3.2 and +1.9 hPa, respectively. This compares to +1.3 and +0.6 hPa for the single-level analysis, that is, a factor of 2.5 to 3 increase. For the NAO, the two-level analysis produces a composite teleconnection of +6.4 hPa for the observations, a factor of 2 increase over the single-level value (+3.1 hPa). In the model simulation, however, the QBO effect obtained is +4.2 hPa, an increase of more than a factor of 6.

While the resampling of the observed and simulated winters using the "deep" QBO phase definition increases the size of the composite differences, it also decreases the number of sample winters in each composite, which could present a challenge for obtaining significance for the signal. Using the same Monte Carlo approach as in previous sections, however, we find that the AO signal is significant at the 99% level for both the observations and the simulation (Figures 7a and 7b). This is a much higher level of confidence than is found in the single-level analysis, in spite of the smaller composite sizes. Similarly, the NAO signal is significant at the 95% level for observations and 99% level for the simulation (Figures 7c and 7d). Composites of each of the other opposite pairs of phases (e.g., P5 minus P1) do not produce significant AO and NAO responses (see Tables 1 and 2).

We now repeat our tests of whether the model response is significantly different to that found in observations using the phase-angle to produce QBO composites. As for the single-level index (Figure 4), we subsample the model simulation by choosing deep QBO-W and QBO-E composites equal in size to those in observations (12 and 11 winters, respectively). The distribution of differences of the means of these composites obtained with 1,000 resamples is shown in Figure 8. For the AO, the distribution of values from trials conditioned on the deep QBO is better separated from the distribution that is not conditioned on the QBO (Figure 8a) than in the single-level case (Figure 4a). The observed AO response lies very close to the 90% limit of the conditional distribution. This means that the frequency with which the model simulates a QBO-AO teleconnection of the same size as in observations is less than in the single-level analysis. It is less likely, therefore, that the model is consistent with reanalysis, and we are close to being able to confidently state (at the 90% level) that the model response (+1.9 hPa) is smaller than the observed response (+3.2 hPa). For the NAO, the observed QBO teleconnection (+6.4 hPa) is less than the 90% limit of the distribution of deep QBO differences in the simulation (Figure 8b), meaning that the model and observations are not statistically distinguishable. This likely arises because of the very large increase in the simulated NAO teleconnection between the two-level QBO (+4.2 hPa) and the single-level QBO (+0.6 hPa) definitions.

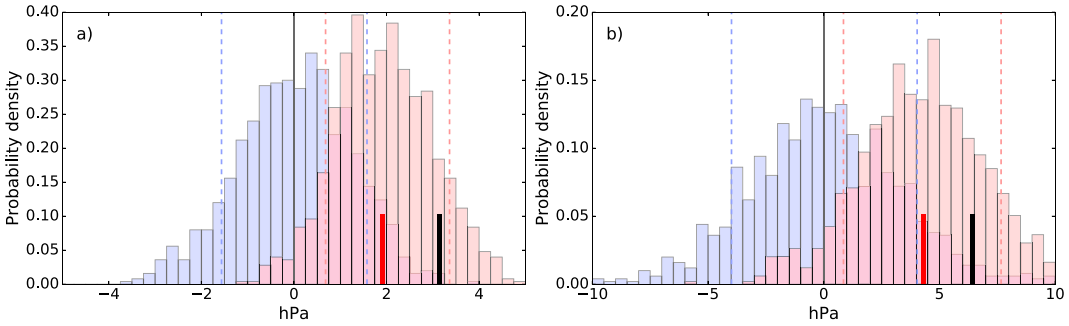


**Figure 8.** Same as in Figure 4 but using the observed sample sizes of P4 and P8 to calculate the distribution of simulated winter (a) AO and (b) NAO responses.

## 4. Discussion and Conclusions

We have tested the robustness of observed QBO influences on the Northern Hemisphere winter circulation and assessed whether model simulations of these teleconnections are consistent with observations. It has long been reported that these responses appear to project strongly onto the main modes of year-to-year NH winter circulation variability, namely, the AO and the NAO, and various mechanistic explanations for these links have been advanced. It is not clear, however, whether the QBO teleconnections seen over the 63-year historical record, or indeed apparent differences with model simulations, are robust. To address these questions, we have used observational data sets of QBO winds and Northern Hemisphere MSLP alongside a long control simulation of a climate model. The model provides a much larger number of winters than the observed data sets (313 versus 63 winters) with which we can gauge the impact of QBO variability on the AO and NAO.

In the first instance, we examined the teleconnections using an index of the QBO specified as the equatorial zonal mean zonal wind at 30 hPa. The observed AO response to the QBO is marginally statistically significant, that is to say, it is unlikely (at the 90% confidence level) that it arises from the chance sampling of unrelated variability. It is likely (but not certain), therefore, that AO variations are partly associated with the QBO as measured by 30-hPa winds. The NAO teleconnection is also on the margins of significance (falling just below the 90% confidence limit), which supports this qualified view of the robustness of the QBO's extratropical teleconnections.

In the much longer model simulation, there is a highly significant (>95%) link between the QBO and the AO. Despite this, the amplitude of the teleconnection is less than half that seen in observations. For the NAO, on the other hand, there is no significant signal. The simulation of a robust connection with the AO, at least, strengthens the case for the observed teleconnection being genuine. However, comparing the simulated and observed amplitudes, we find that we cannot reliably conclude that there is a difference, since estimates of the simulated teleconnection using the same number of winters as available in observations are too often similar to that found in the observational record. In the case of the NAO, the response is not significant, being just below the 90% confidence threshold. This is because the model response is so small it is essentially absent. Nevertheless, we conclude that the 63-year observational record is not long enough to discriminate between the model and observed QBO teleconnections. This is perhaps not surprising given that the observed teleconnections with the 30-hPa QBO metric often used in such analyses are only just significant over this period. Clearly, a longer observational record would reduce the level of contamination of the estimates by variability in the AO and NAO indices, as shown by the greater resolution of signals in the multicentury simulation.

As an alternative to a single-level QBO index, we examined a definition based on the zonal mean zonal winds at 15 and 30 hPa. In the space spanned by the variability at these two levels, we were able to identify winters with the greatest midstratospheric vertical extent of QBO-W and QBO-E phases. Compositing the AO and NAO based on this definition showed increased estimates of the magnitude of QBO influence in both observations and the model simulation. In the observed case, the estimated AO and NAO amplitudes are a large fraction of the standard deviations of year-to-year variability, suggesting a substantial impact of the QBO on Northern Hemisphere winter circulation. In addition, both observed and simulated AO and NAO signals are significant above the 95% level. Despite the qualified identification of a QBO influence from the single-level analysis, therefore, we conclude from this alternative analysis that robust associations with the AO and NAO exist. For the model simulation, although AO signals were found using both metrics of the QBO, the two-level analysis reveals an NAO teleconnection that is absent from the single-level analysis.

The two-level analysis of the AO link with the QBO is better at discriminating between the strength of the observed and simulated effect, such that the difference is close to being significant at the 90% level. This suggests (further to the analysis of the NAO with the single-level index) that the model produces atmospheric circulation signals associated with the QBO that are too weak. The simulated AO teleconnection strength is nominally about half of that inferred from observations, but this estimate is clearly associated with substantial uncertainty given the natural variability of the AO, which is reflected in the width of the distribution in Figure 8a. The difference between the NAO teleconnections obtained from the two-level analysis is not significant.

In demonstrating robust links between the QBO and wintertime Northern Hemisphere atmospheric circulation indices, we are not able to formally identify the causal relationships between different parts of the climate system. Given past work on the mechanisms of QBO influences on the extratropical atmosphere (for example, Anstey & Shepherd, 2014; Dunkerton & Baldwin, 1991; Garfinkel & Hartmann, 2011; Hamilton, 1998; Holton & Tan, 1980, 1982), it is likely that the associations found here represent a physical response of the AO and NAO to driving by the QBO. While this seems the most likely possibility, our results may also be consistent with the QBO and Northern Hemisphere circulation being influenced by a third, unidentified, factor. In this case, it would be possible to have stable long-term statistical association without any direct physical link.

The finding that QBO phases spanning the range of the equatorial midstratosphere produce stronger AO and NAO signals (both using observations and in the model) is intriguing. The single-level index represents only part of the information comprising the two-level metric, so it is not expected that the addition of the extra level is simply acting to smooth out random noise. The stronger AO and NAO signals associated with vertical coherence of the QBO phases identified by the two-level metric are, however, consistent with the Holton-Tan hypothesis, which suggests that the QBO phase modulates the amounts of upward propagating NH planetary wave flux penetrating the tropics and being steered toward the stratospheric polar vortex. If a particular QBO phase has a deeper vertical extent, therefore, then the mechanism will operate over a broader vertical range, and perhaps have a greater integrated effect on the polar vortex. This might be important for the long-wavelength planetary waves thought to be important for this mechanism, which also have large vertical wavelengths. Examination of aspects of the mechanistic connections behind the statistical QBO teleconnections could be a further use of the multicentury simulation in future work. This would also be necessary to understand the causes of the weakness of the simulated QBO influence compared to that inferred from observations.

In summary, we have shown that there is a robust QBO teleconnection to Northern Hemisphere winter extratropical surface climate but simulated teleconnections are likely weaker than observed. Categorization of QBO phases using equatorial winds over a range of stratospheric levels is required to maximize the inferred amplitude and the ability to detect QBO signals. This approach reveals a QBO effect that is a larger fraction of the total winter circulation variability, and suggests that the QBO may be one of the major drivers of year-to-year variability in seasonal conditions for parts of the Northern Hemisphere. The smaller signal in the model is reminiscent of weak winter circulation responses seen in other contexts, such as to the solar cycle and volcanic eruptions (Driscoll et al., 2012; Misios et al., 2016), and the smaller-than-expected amplitude of seasonal NAO predictions (Dunstone et al., 2016; Eade et al., 2014; Scaife, Arribas, et al., 2014; Scaife, Athanassiadou, et al., 2014). This is consistent with a much broader "signal-to-noise" problem (Eade et al., 2014) that may not be specific to the QBO teleconnection itself. Nevertheless, we conclude that seasonal and decadal climate forecasts of Northern Hemisphere winter would be made more skillful by better representation and predictability of the QBO and improvements in the realism of its teleconnections.

**Acknowledgments**
M.B.A., J.R.K., and A.A.S were supported by the UK-China Research & Innovation Partnership Fund through the Met Office Climate Science for Service Partnership (CSSP) China as part of the Newton Fund. This work was supported by the Joint DECC/Defra Met Office Hadley Centre Climate Programme (GA01101). Y.L. and T.W. were supported by the National Key Research and Development Program of China (2016YFA0602100). L.J.G. was supported by the UK Natural Environment Research Council (NERC) through the National Centre for Atmospheric Science (NCAS). The authors would like to thank the following for their valuable contributions to early discussions regarding the analysis of the QBO: Scott Osprey, Neal Butchart, Andrew Bushell, and Sarah Ineson. The winter MSLP and QBO data for the HadGEM3-GC2 preindustrial control run are available to download (Andrews, 2018).

## References

Andrews, M. B. (2018). "Data for Publication, 'Observed and Simulated Teleconnections between the Stratospheric Quasi-Biennial Oscillation and Northern Hemisphere Winter Atmospheric circulation' (version 2018.11.20)". https://doi.org/10.5281/zenodo.1492251

Andrews, M. B., Knight, J. R., & Gray, L. J. (2015). A simulated lagged response of the North Atlantic Oscillation to the solar cycle over the period 1960–2009. *Environmental Research Letters*, *10*(5), 054022. https://doi.org/10.1088/1748-9326/10/5/054022

Anstey, J. A., & Shepherd, T. G. (2014). High-latitude influence of the Quasi-Biennial Oscillation. *Quarterly Journal of the Royal Meteorological Society*, *140*, 1–21. https://doi.org/10.1002/qj.2132

Baldwin, M. P., & Dunkerton, T. J. (2001). Stratospheric harbingers of anomalous weather regimes. *Science*, *294*(5542), 581–584. https://doi.org/10.1126/science.1063315

Baldwin, M. P., Gray, L. J., Dunkerton, T. J., Hamilton, K., Haynes, P. H., Randel, W. J., et al. (2001). The Quasi-Biennial Oscillation. *Reviews of Geophysics*, *39*(2), 179–229. https://doi.org/10.1029/1999RG000073

Bell, C. J., Gray, L. J., Charlton-Perez, A. J., Joshi, M. M., & Scaife, A. A. (2009). Stratospheric communication of El Niño teleconnections to European winter. *Journal of Climate*, *22*(15), 4083–4096. https://doi.org/10.1175/2009JCLI2717.1

Driscoll, S., Bozzo, A., Gray, L. J., Robock, A., & Stenchikov, G. (2012). Coupled Model Intercomparison Project 5 (CMIP5) simulations of climate following volcanic eruptions. *Geophysical Research*, *117*, D17105. https://doi.org/10.1029/2012JD017607

Dunkerton, T. J. (2017). Near identical cycles of the Quasi-Biennial Oscillation in the equatorial lower stratosphere. *Journal of Geophysical Research: Atmospheres*, *122*, 8467–8493. https://doi.org/10.1002/2017JD026542

Dunkerton, T. J., & Baldwin, M. P. (1991). Quasi-biennial modulation of planetary wave fluxes in the northern hemisphere winter. *Journal of the Atmospheric Sciences*, *48*(8), 1043–1061. https://doi.org/10.1175/1520-0469(1991)048<1043:QBMOPW>2.0.CO;2

Dunkerton, T. J., Delisi, D. P., & Baldwin, M. P. (1988). Distribution of major stratospheric warmings in relation to the Quasi-Biennial Oscillation. *Geophysical Research Letters*, *15*(2), 136–139. https://doi.org/10.1029/GL015i002p00136

Dunstone, N., Smith, D., Scaife, A., Hermanson, L., Eade, R., Robinson, N., et al. (2016). Skilful predictions of the winter North Atlantic Oscillation one year ahead. *Nature Geoscience*, *9*(11), 809–814. https://doi.org/10.1038/ngeo2824

Eade, R., Smith, D., Scaife, A., Wallace, E., Dunstone, N., Hermanson, L., & Robinson, N. (2014). Do seasonal-to-decadal climate predictions underestimate the predictability of the real world? *Geophysical Research Letters*, *41*, 5620–5628. https://doi.org/10.1002/2014GL061146

Ebdon, R. A. (1975). The Quasi-Biennial Oscillation and its association with tropospheric circulation patterns. *Meteorological Magazine*, *104*, 282–297.

Fraedrich, K., Pawson, S., & Wang, R. (1993). An EOF analysis of the vertical-time delay structure of the Quasi-Biennial Oscillation. *Journal of the Atmospheric Sciences*, *50*(20), 3357–3365. https://doi.org/10.1175/1520-0469(1993)050<3357:AEAOTV>2.0.CO;2

Garfinkel, C. I., & Hartmann, D. L. (2011). The influence of the Quasi-Biennial Oscillation on the troposphere in winter in a hierarchy of models. Part I: Simplified dry GCMs. *Journal of the Atmospheric Sciences*, *68*(6), 1273–1289. https://doi.org/10.1175/2011JAS3665.1

Gong, D.-Y., Wang, S.-W., & Zhu, J.-H. (2001). East Asian winter monsoon and Arctic oscillation. *Geophysical Research Letters*, *28*(10), 2073–2076. https://doi.org/10.1029/2000GL012311

Gray, L. J., Anstey, J. A., Kawatani, Y., Lu, H., Osprey, S., & Schenzinger, V. (2018). Surface impacts of the Quasi-Biennial Oscillation. *Atmospheric Chemistry and Physics*, *18*(11), 8227–8247. https://doi.org/10.5194/acp-18-8227-2018

Gray, L. J., Beer, J., Geller, M., Haigh, J. D., Lockwood, M., Matthes, K., et al. (2010). Solar influences on climate. *Reviews of Geophysics*, *48*, RG4001. https://doi.org/10.1029/2009RG000282

Gray, L. J., Scaife, A. A., Mitchell, D. M., Osprey, S., Ineson, S., Hardiman, S., et al. (2013). A lagged response to the 11 year solar cycle in observed winter Atlantic/European weather patterns. *Journal of Geophysical Research: Atmospheres*, *118*, 13,405–13,420. https://doi.org/10.1002/2013JD020062

Gray, L. J., Woollings, T. J., Andrews, M. B., & Knight, J. K. (2016). Eleven-year solar cycle signal in the NAO and Atlantic/European blocking. *Quarterly Journal of the Royal Meteorological Society*, *142*(698), 1890–1903. https://doi.org/10.1002/qj.2782

Hamilton, K. (1998). Effects of an imposed Quasi-Biennial Oscillation in a comprehensive troposphere-stratosphere-mesosphere general circulation model. *Journal of the Atmospheric Sciences*, *55*(14), 2393–2418. https://doi.org/10.1175/1520-0469(1998)055<2393:EOAIQB>2.0.CO;2

Holton, J. R., & Tan, H.-C. (1980). The influence of the equatorial Quasi-Biennial Oscillation on the global circulation at 50 mb. *Journal of the Atmospheric Sciences*, *37*(10), 2200–2208. https://doi.org/10.1175/1520-0469(1980)037<2200:TIOTEQ>2.0.CO;2

Holton, J. R., & Tan, H.-C. (1982). The Quasi-Biennial Oscillation in the northern hemisphere lower stratosphere. *Journal of the Meteorological Society of Japan*, *60*(1), 140–148. https://doi.org/10.2151/jmsj1965.60.1_140

Hurrell, J. W., Kushnir, Y., Ottersen, G., & Visbeck, M. (2003). The North Atlantic Oscillation: Climate significance and environmental impact. *Geophysical Monograph Series*, *134*, 1–36.

Ineson, S., Scaife, A. A., Knight, J. R., Manners, J. C., Dunstone, N. J., Gray, L. J., & Haigh, J. D. (2011). Solar forcing of winter climate variability in the northern hemisphere. *Nature Geoscience*, *4*(11), 753–757. https://doi.org/10.1038/ngeo1282

Jones, C. D., Hughes, J. K., Bellouin, N., Hardiman, S. C., Jones, G. S., Knight, J., et al. (2011). The HadGEM2-ES implementation of CMIP5 centennial simulations. *Geoscientific Model Development*, *4*(3), 543–570. https://doi.org/10.5194/gmd-4-543-2011

Kalnay, E., Kanamitsu, M., Kistler, R., Collins, W., Deaven, D., Gandin, L., et al. (1996). The NCEP/NCAR 40-year reanalysis project. *Bulletin of the American Meteorological Society*, *77*(3), 437–471. https://doi.org/10.1175/1520-0477(1996)077<0437:TNYRP>2.0.CO;2

Kidston, J., Scaife, A. A., Hardiman, S. C., Mitchell, D. M., Butchart, N., Baldwin, M. P., & Gray, L. J. (2015). Stratospheric influence on tropospheric jet streams, storm tracks and surface weather. *Nature Geoscience*, *8*(6), 433–440. https://doi.org/10.1038/NGEO2424

Kodera, K., Mukougawa, H., Maury, P., Ueda, M., & Claud, C. (2016). Absorbing and reflecting sudden stratospheric warming events and their relationship with tropospheric circulation. *Journal of Geophysical Research: Atmospheres*, *121*, 80–94. https://doi.org/10.1002/2015JD023359

Kolstad, E. W., Breiteig, T., & Scaife, A. A. (2010). The association between stratospheric weak polar vortex events and cold air outbreaks in the northern hemisphere. *Quarterly Journal of the Royal Meteorological Society*, *136*(649), 886–893. https://doi.org/10.1002/qj.620

Kunze, M. (2017). QBO dataseries. Retrieved from http://www.geo.fu-berlin.de/en/met/ag/strat/produkte/qbo/index.html

Liess, S., & Geller, M. A. (2012). On the relationship between the QBO and distribution of tropical deep convection. *Journal of Geophysical Research*, *117*, D03108. https://doi.org/10.1029/2011JD016317

Madec, G. (2008). NEMO ocean engine, Tech. Rep. 27, Note du Pole de modélisation, Institut Pierre-Simon Laplace (IPSL).

Marshall, A. G., & Scaife, A. A. (2009). Impact of the QBO on surface winter climate. *Journal of Geophysical Research*, *114*, D18110. https://doi.org/10.1029/2009JD011737

Misios, S., Mitchell, D. M., Gray, L. J., Tourpali, K., Matthes, K., Hood, L., et al. (2016). Solar signals in CMIP-5 simulations: Effects of atmosphere-ocean coupling. *Quarterly Journal of the Royal Meteorological Society*, *142*, 928–941. https://doi.org/10.1002/qj.2695

Newman, P. A., Coy, L., Pawson, S., & Lait, L. R. (2016). The anomalous change in the QBO in 2015–16. *Geophysical Research Letters*, *43*, 8791–8797. https://doi.org/10.1002/2016GL070373

Osprey, S. M., Butchart, N., Knight, J. R., Scaife, A. A., Hamilton, K., Anstey, J. A., et al. (2016). An unexpected disruption of the atmospheric Quasi-Biennial Oscillation. *Science*, *353*(6306), 1424–1427. https://doi.org/10.1126/science.aah4156

Pascoe, C. L., Gray, L. J., & Scaife, A. A. (2006). A GCM study of the influence of equatorial winds on the timing of sudden stratospheric warmings. *Geophysical Research Letters*, *33*, L06825. https://doi.org/10.1029/2005GL024715

Reed, R. J., Campbell, W. J., Rasmussen, L. A., & Rogers, D. G. (1961). Evidence of a downward-propagating annual wind reversal in the equatorial stratosphere. *Journal of Geophysical Research*, *66*(3), 813–818. https://doi.org/10.1029/JZ066i003p00813

Ruti, P. M., Lucarini, V., Dell'Aquila, A., Calmanti, S., & Speranza, A. (2006). Does the subtropical jet catalyze the midlatitude atmospheric regimes? *Geophysical Research Letters*, *33*, L06814. https://doi.org/10.1029/2005GL024620

Sato, M., Hansen, J. E., McCormick, M. P., & Pollack, J. B. (1993). Stratospheric aerosol optical depths, 1850–1990. *Journal of Geophysical Research*, *98*(D12), 22,987–22,994. https://doi.org/10.1029/93JD02553

Scaife, A. A., Arribas, A., Blockley, E., Brookshaw, A., Clark, R. T., Dunstone, N., et al. (2014). Skillful long-range prediction of European and North American winters. *Geophysical Research Letters*, *41*, 2514–2519. https://doi.org/10.1002/2014GL059637

Scaife, A. A., Athanassiadou, M., Andrews, M., Arribas, A., Baldwin, M., Dunstone, N., et al. (2014). Predictability of the Quasi-Biennial Oscillation and its northern winter teleconnection on seasonal to decadal timescales. *Geophysical Research Letters*, *41*, 1752–1758. https://doi.org/10.1002/2013GL059160

Scaife, A. A., Butchart, N., Warner, C. D., & Swinbank, R. (2002). Impact of a spectral gravity wave parameterization on the stratosphere in the Met Office unified model. *Journal of the Atmospheric Sciences*, *59*(9), 1473–1489. https://doi.org/10.1175/1520-0469(2002)059<1473:IOASGW>2.0.CO;2

Scaife, A. A., Ineson, S., Knight, J. R., Gray, L., Kodera, K., & Smith, D. M. (2013). A mechanism for lagged North Atlantic climate response to solar variability. *Geophysical Research Letters*, *40*, 434–439. https://doi.org/10.1002/grl.50099

Schenzinger, V. (2017). Tropical stratosphere variability and extratropical teleconnections, DPhil. Thesis, Oxford University (pp. 180).

Scherhag, R. (1952). Die explosionsartige Stratosphärenerwärmung des Spätwinters 1951/52. *Berichte der Deutschen Wetterdienstes*, *38*, 51–63.

Simpson, I. R., Blackburn, M., & Haigh, J. D. (2009). The role of eddies in driving the tropospheric response to stratospheric heating perturbations. *Journal of the Atmospheric Sciences*, *66*(5), 1347–1365. https://doi.org/10.1175/2008JAS2758.1

Stenchikov, G., Hamilton, K., Robock, A., Ramaswamy, R., & Daniel Schwarzkopf, M. (2004). Arctic oscillation response to the 1991 Pinatubo eruption in the SKYHI general circulation model with a realistic Quasi-Biennial Oscillation. *Journal of Geophysical Research*, *109*, D03112. https://doi.org/10.1029/2003JD003699

Thompson, D. W. J., & Wallace, J. M. (1998). The Arctic oscillation signature in the wintertime geopotential height and temperature fields. *Geophysical Research Letters*, *25*(9), 1297–1300. https://doi.org/10.1029/98GL00950

Thompson, D. W. J., & Wallace, J. M. (2001). Regional climate impacts of the northern hemisphere annular mode. *Science*, *293*(5527), 85–89. https://doi.org/10.1126/science.1058958

Valcke, S. (2010). The OASIS3 coupler: A European climate modelling community software. *Geoscientific Model Development*, *6*(2), 373–388. https://doi.org/10.5194/gmd-6-373-2013

Veryard, R. G., & Ebdon, R. A. (1961). Fluctuations in tropical stratospheric winds. *Meteorological Magazine*, *90*, 125–143.

Wallace, J. M., Panetta, R. L., & Estberg, J. (1993). Representation of the equatorial stratospheric Quasi-Biennial Oscillation in EOF phase space. *Journal of the Atmospheric Sciences*, *50*(12), 1751–1762. https://doi.org/10.1175/1520-0469

Williams, K. D., Harris, C. M., Bodas-Salcedo, A., Camp, J., Comer, R. E., Copsey, D., et al. (2015). The Met Office global coupled model 2.0 (GC2) configuration. *Geoscientific Model Development*, *88*, 1509–1524. https://doi.org/10.5194/gmd-88-1509-2015